Proceedings of the 12th International Conference on Quasicrystals (ICQ12)

Characterization of Rapidly Solidified $Al_{65}Cu_{20}Fe_{15}$ Alloy in Form of Powder or Ribbon

L. Lityńska-Dobrzyńska[a,*], J. Dutkiewicz[a], K. Stan-Głowińska[a], L. Dembinski[b], C. Coddet[b] and P. Ochin[c]

[a]Institute of Metallurgy and Materials Science, Polish Academy of Sciences
W.S. Reymonta 25, 30-059 Kraków, Poland

[b]Université de Technologie de Belfort-Montbeliard, Site de Sevenans, 90010, Belfort, France

[c]Institut de Chimie et des Matériaux Paris Est, CNRS-Université Paris XII
2-8 rue Henri Dunant, 94320 Thiais, France

The $Al_{65}Cu_{20}Fe_{15}$ alloy has been prepared by conventional casting to the mould and by melt spinning or atomisation techniques. The melt spun ribbon was in the form of fragmented, brittle flakes, atomized powder has spherical shape with average size 17.2 μm. It was found that icosahedral I-phase was the main phase in all types of prepared samples. In the conventionally cast alloy the following phases have been identified additionally: λ-$Al_{13}Fe_4$, τ-AlCu(Fe) and η_2-AlCu. In the melt-spun ribbon the formation of η_2 is avoided, while in the atomised powder the I-phase coexists with small amount of copper rich τ-phase. In the cast ingot the I-phase form as a product of peritectic reaction $\lambda + L$, while in the ribbon and in the powder quasicrystal solidified from the undercooled melt as primary phase and next metastable cubic τ-AlCu(Fe) was formed at the interdendritic areas. Single I-phase grains of the sizes about 1 μm are observed in the ribbon close to the wheel side.

DOI: 10.12693/APhysPolA.126.512

PACS: 81.05.Bx, 81.30.−t, 61.44.Br, 61.05.cp, 61.05.jm

1. Introduction

Al–Cu–Fe quasicrystalline alloys exhibit unique combination of physical, thermal, and mechanical properties. Due to their thermodynamic stability, non-toxicity and low cost of their alloying elements they have potential for practical applications [1, 2]. Stable icosahedral quasicrystalline phase (I-phase) lies in very narrow composition range in ternary Al–Cu–Fe system [3, 4] and usually it coexists with other phases in cast alloys. For instance, quasicrystalline as well as crystalline faceted single grains of four phases were obtained during directional crystallization of an alloy by the Bridgman technique [5].

The solidification sequence of the quasicrystal forming Al–Cu–Fe alloys depends on chemical composition and solidification rates. It has been already shown that the I-phase forms by peritectic reaction $L + \lambda + \beta \rightarrow$ I-phase at slow and moderate cooling rates [6, 7]. Usually the reaction is not completed and other crystalline phases can form. A broader area for quasicrystalline structure can be formed in rapidly solidified alloys and indeed single I-phase structure was observed in the rapidly solidified $Al_{65}Cu_{20}Fe_{15}$ ribbon [8, 9]. However, for the same composition the single quasicrystalline phase cannot be obtained by using the cooling rate 5–7 $\times$ 10^4 deg/s and the ribbons exhibit two- or three-phase microstructure [7, 10]. In the case of ribbons quasicrystals solidified directly from the melt as primary phase and crystalline phases formed at the inter-dendritic region from the remaining melt [7]. It was shown also that a single I-phase can be obtained by annealing at 600–800 °C around the alloy composition $Al_{64}Cu_{24}Fe_{12}$–$Al_{61.75}Cu_{25.5}Fe_{12.75}$ [11].

Although there have been many investigations concerning the alloys solidified with different cooling rates, the results are not consistent. In the present study, the microstructural characteristic of rapidly solidified $Al_{65}Cu_{20}Fe_{15}$ alloy obtained by two methods: melt spinning (ribbon) and by atomization (powder) have been done and compared to the conventionally cast alloy.

2. Experimental

The $Al_{65}Cu_{20}Fe_{15}$ (in at.%) alloy were prepared by induction melting under argon atmosphere using Al, Cu, and Fe elements of purity 99.99%. The cast alloy was used as an initial material for rapidly solidified ribbon and atomized powder. Ribbon was produced using a melt-spinning technique under helium atmosphere. In this process melted alloy was ejected onto a copper wheel rotating at linear velocity v = 20 m/s. The pressure of the gas ejecting the molten alloy was 180 mbar. The obtained ribbon was in the form of fragmented, brittle flakes. The powders were prepared by gas atomization device under argon using Rayleigh-plateau forces in primary mode. The estimated cooling rate for the ribbon and for the atomized powder was in the range 10^5–10^6 K/s.

The microstructure of the conventionally cast alloy, melt spun ribbon, and atomized powder was examined using Philips PW 1840 X-ray diffractometer (XRD) with Cu K_α radiation (λ = 1.5406 Å), FEI scanning electron microscope E-SEM XL30 (SEM) and FEI transmission electron microscope Tecnai G^2 (TEM) operating at 200 keV equipped with high-angle annular dark field scanning transmission electron microscopy detector

*corresponding author; e-mail: l.litynska@imim.pl

(HAADF-STEM) combined with energy dispersive X-ray (EDX) EDAX microanalysis. In the case of the ribbon Tenupol-5 double jet electropolisher was used for the thin foil preparation in an electrolyte containing nitric acid and methanol (1:3) at the temperature of $-30\,^{\circ}C$ and voltage of 15 V. In order to prepare the TEM samples from atomized powder, thin slices of the powder embedded in kit were cut with Leica EM UC6 ultramicrotome using diamond knife. Then thin slices were placed on a carbon film supported by a nickel grid.

3. Results and discussion

The X-ray diffraction pattern (upper curve in Fig. 1) revealed that there are three main phases in the cast ingot: icosahedral I-phase, monoclinic λ-$Al_{13}Fe_4$ (space group $C2/m$, $a = 1.5489$ nm, $b = 0.80831$ nm, $c = 1.2476$ nm, $\beta = 107.72°$) and cubic β (or τ) Al(Cu,Fe) (space group $Pm3m$, $a = 0.29$ nm). Both phases, iron rich β and low temperature, copper rich τ (denotes also as β' in [6]) have similar lattice constants and the X-ray is not suitable to distinguish them.

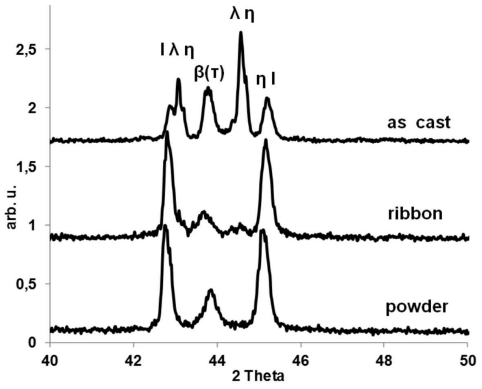

Fig. 1. X-ray patterns of as cast, melt spun ribbon, and atomized powder of $Al_{65}Cu_{20}Fe_{15}$ alloy.

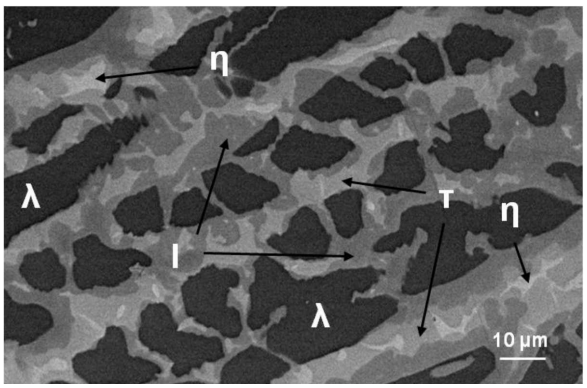

Fig. 2. SEM image of the $Al_{65}Cu_{20}Fe_{15}$ cast alloy.

High temperature β-AlFe(Cu) is stable while the copper rich τ-AlCu(Fe) is metastable and forms at the later stage of solidification at the interdendritic region. Additional weak reflections present in the X-ray pattern could be identified as low temperature modification of the η_2-AlCu (space group $I12/m1$, $a = 0.9889$ nm, $b = 0.4105$ nm, $c = 0.6913$ nm, $\beta = 89.99°$). Distribution of phases identified by X-ray was visible in SEM image in Fig. 2. Dark gray phase was identified by EDX microanalysis as the λ phase, which forms as primary phase from the melt. The grey phase corresponds to the peritectically solidified I-phase while the light-grey phase could be identified as copper rich cubic τ-AlCu(Fe). The light phase lying inside the τ-phase with slightly different composition corresponds to the η_2 phase.

The mean compositions of the phases obtained by EDX microanalysis in SEM (errors were calculated as standard deviations of the obtained results for each phase) as well as the range of composition are shown in Table.

TABLE

Chemical compositions of the phases observed in cast alloys, ribbons and atomized powder. The composition range for each phase is also included.

Phase	Al [at.%]		Cu [at.%]		Fe [at.%]	
	Composition range	Mean value	Composition range	Mean value	Composition range	Mean value
Cast alloy						
λ	69.6–70.0	69.9 ± 0.2	4.3–5.2	4.8 ± 0.4	25.2–25.7	25.4 ± 0.3
I	62.3–62.9	62.5 ± 0.3	23.4–25.1	24.3 ± 0.8	12.6–13.7	13.2 ± 0.5
τ	50.5–51.3	51.0 ± 0.4	43.8–45.2	44.5 ± 0.7	4.2–4.9	4.5 ± 0.4
η	46.8–47.5	47.1 ± 0.4	50.4–51.3	50.9 ± 0.5	1.9–2.1	2.0 ± 0.1
Ribbon						
I	63.3–68.6	66.9 ± 1.3	12.7–18.3	16.2 ± 2.0	14.7–19.6	16.8 ± 1.9
λ	71.5–72.8	72.1 ± 0.9	5.6–6.6	6.1 ± 0.7	20.5–22.8	21.7 ± 1.6
τ	40.3–40.6	40.5 ± 0.2	53.6–55.5	54.5 ± 1.3	3.9–6.1	5.0 ± 1.5
Atomized powder						
I	62.3–68.3	66.0 ± 1.3	15.2–19.9	17.2 ± 1.9	14.2–18.6	16.8 ± 1.4
τ	42.5–44.0	43.1 ± 0.6	52.5–55.5	54.2 ± 1.3	1.2–4.9	2.7 ± 1.7

Similar sequence of phases in $Al_{65}Cu_{20}Fe_{15}$ has been observed by Cheung et al. [12] although the crystal structure of the copper rich phase with the composition related to η_2 was not described. It was found also that for the same alloy composition the Θ-Al_2Cu phase could solidify together with the τ-phase instead of the η_2 [13].

The η_2 phase has been observed in the number of AlCuFe cast alloys with Fe content in the range 7.5–17.85 at.% and copper content in the range 12.5–31 at.%, as final stage of solidification of remaining liquid [6]. The first-principles calculations showed that the η_2 phase is stable at concentrations less than 2.5% Fe due to iron localization in the copper sublattice and coexist with τ-AlCu(Fe) phase [14].

In the rapidly solidified ribbon the amount of phases was reduced as compared to the alloy cast as an ingot and only reflections related to the I-phase, τ and λ were observed in X-ray pattern (Fig. 1). The SEM image of the cross-section of the ribbon showed that it consists mainly of the cell or dendrites (grey phase) of the I-phase surrounded by light in contrast τ-phase (Fig. 3). Particles of a light grey contrast corresponding probably to the λ-phase could be also noticed. The microstructure is not homogeneous and the area of small grains are located near the wheel side of the ribbons. The TEM observation confirmed the presence of two regions inside the ribbon.

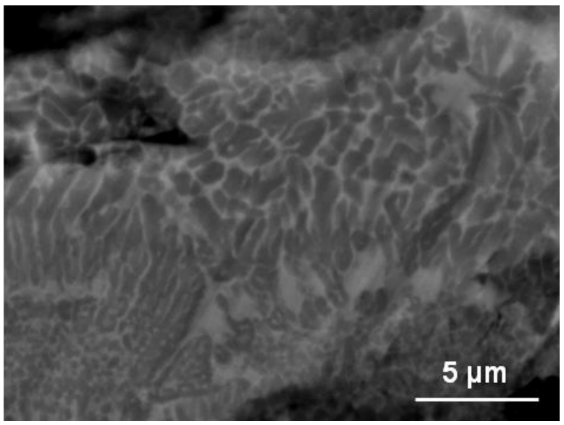

Fig. 3. SEM image of the cross-section of $Al_{65}Cu_{20}Fe_{15}$ ribbon.

The microstructure presented in Fig. 4a shows the cell of the I-phase and the τ-phase in inter-cell areas. The crystal structure of both phases were identified by selected area diffraction patterns (SADP) and the example of SADP obtained for τ-phase with zone axis [111] is inserted in Fig. 4a. The λ particles with characteristic stacking faults in the 010 planes, surrounded by I-phase are presented in Fig. 4b, together with corresponding SADP. Similar morphology of the λ particles was observed also in the $Al_{66}Cu_{21}Fe_{13}$ ribbon [15].

The second type of microstructure found in investigated ribbon consists of the small grains of the I-phase with sizes approximately 1 μm (Fig. 5). Only I-phase

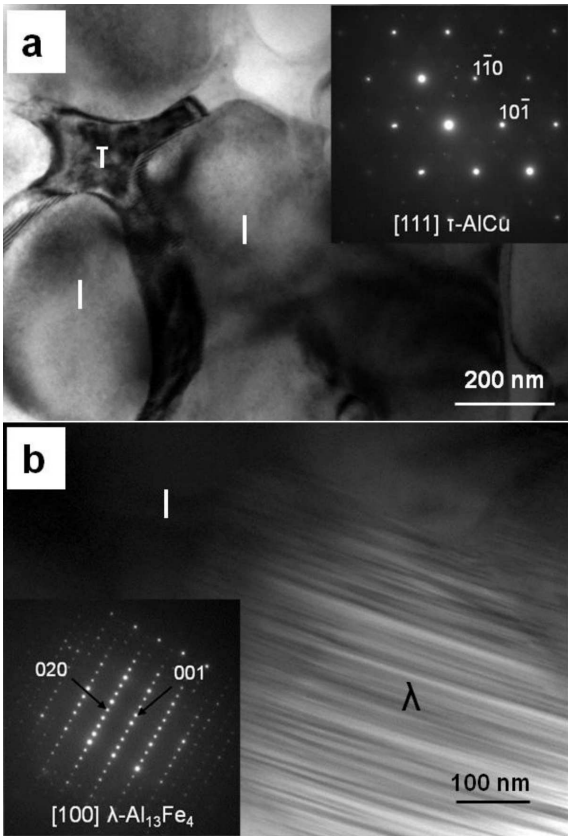

Fig. 4. TEM bright-field image of the $Al_{65}Cu_{20}Fe_{15}$ ribbon of (a) cell of I-phase and τ phase located at inter-cell areas; inserted SADP obtained for the τ-phase, (b) particle of the λ-phase and corresponding SADP.

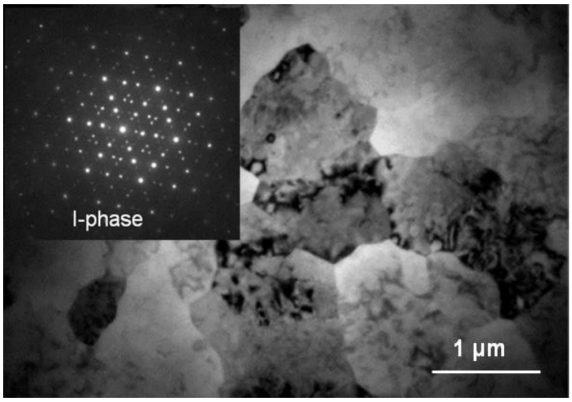

Fig. 5. TEM bright-field image of the $Al_{65}Cu_{20}Fe_{15}$ ribbon and SADP obtained from one grain of the I-phase (3-fold symmetry).

have been identified based on the SADP (as an example threefold icosahedral electron diffraction obtained for one of the grains is inserted in Fig. 5). All phases found in the ribbon were analysed by EDX in TEM to get information of their composition. The EDX results are shown in Table. It could be concluded that part of the ribbon which solidified first at the highest cooling rate contains single I-phase.

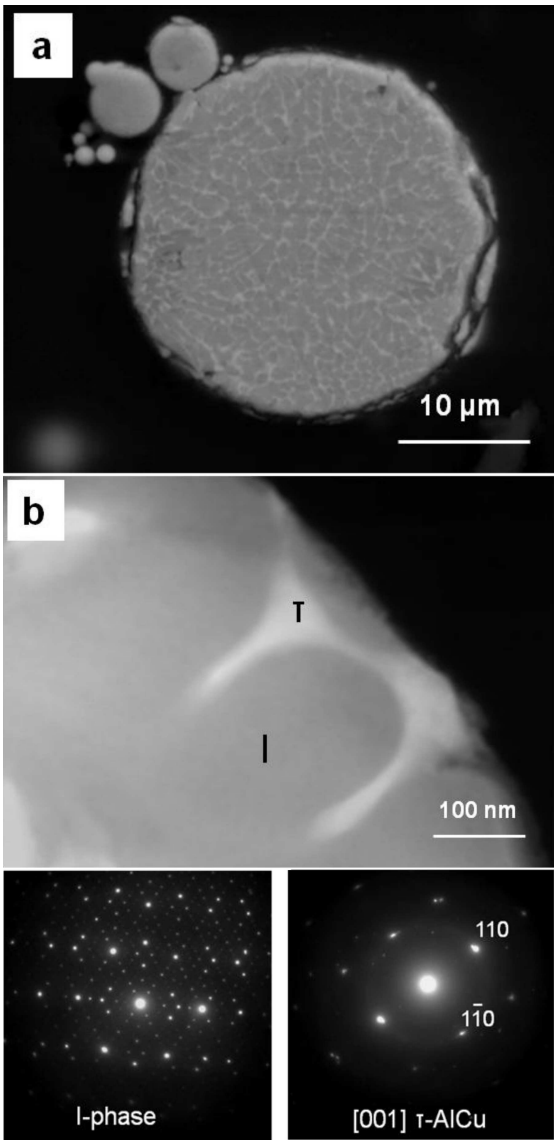

Fig. 6. (a) SEM image of the cross-section of the atomized powder of the $Al_{65}Cu_{20}Fe_{15}$ alloy and (b) STEM-HAADF image and selected area electron diffraction patterns from the dendrite of I-phase (3-fold symmetry) and τ-AlCu phase located at interdendritic areas.

The morphology of atomized powder is spherical, the particle size distribution had a single mode as lognormal Gaussian curve with the average diameter of 17.4 μm. Figure 6a shows SEM image of as-atomized powder cross-section. The microstructure of the powder is similar to that of the melt spun ribbon and consists of homogeneously distributed dendrite of the I-phase and τ-phase in interdendritic areas.

Two phase microstructure is confirmed by X-ray pattern presented in Fig. 1. The chemical composition of the both phases measured by EDX in TEM are shown in Table. The HAADF-STEM image of the powder particle is presented in Fig. 6b, where light phase was identified as τ-phase, while the grey areas correspond to the I-phase. The phase identification was confirmed by electron diffraction. In Fig. 6b the SADPs corresponded to icosahedral dendrite with 3-fold symmetry and to the cubic τ-phase located between dendrite are presented.

4. Conclusion

The icosahedral I-phase was the main phase in cast ingot, melt spun ribbon, and atomized powder of the $Al_{65}Cu_{20}Fe_{15}$ alloy. The highest amount of this phase was observed in ribbon and atomized powder prepared at the highest solidification rate. The ribbon is more inhomogeneous due to variable cooling rate across its cross-section (highest in the wheel side).

In the conventionally cast alloy, besides the I-phase, the following phases have been identified: λ-$Al_{13}Fe_4$, τ-AlCu(Fe) and η_2-AlCu. In the melt-spun rapidly solidified ribbon the formation of η_2-AlCu phase is avoided, while in the atomised powder the I-phase coexists only with copper rich τ-AlCu(Fe) phase.

In cast ingot the icosahedral phase was formed by peritectic reaction. In the melt-spun ribbon and atomised powder quasicrystal solidified as primary phase from the undercooled melt in the form of dendrites or cells. The amount of cubic τ-AlCu was reduced with an increase of the cooling rate (near the wheel side of the ribbon and with decrease of the size of atomised powder particles).

Acknowledgments

Financial support from the Polish National Science Centre NCN (research projects no. 2011/03/B/ST8/05165 and 2011/01/M/ST8/07828) is gratefully acknowledged.

References

[1] E. Huttunen-Saaivirta, *J. Alloys Comp.* **363**, 150 (2004).

[2] J.M. Dubois, *Chem. Soc. Rev.* **41**, 6760 (2012).

[3] M. Quiquandon, A. Quivy, J. Devaud, F. Faudot, S. Lefebvre, M. Bessière, Y. Calvayrac, *J. Phys., Condens. Matter* **8**, 2487 (1996).

[4] L. Zhang, R. Lück, *J. Alloys Comp.* **342**, 53 (2002).

[5] M. Surowiec, W. Bogdanowicz, J. Krawczyk, B. Formanek, M. Sozanska, *Philos. Mag.* **91**, 2458 (2011).

[6] L. Zhang, R. Lück, *Z. Metallkd.* **94**, 774 (2003).

[7] S.M. Lee, H.J. Jeon, B.H. Kim, W.T. Kim, D.H. Kim, *Mater. Sci. Eng. A* **304-306**, 871 (2001).

[8] A.P. Tsai, A. Inoue, T. Masumoto, *J. Mater. Sci. Lett.* **6**, 1403 (1987).

[9] B. Avar, M. Gogebakan, F. Yilmaz, *Z. Kristallogr.* **223**, 731 (2008).

[10] E. Huttunen-Saarivita, J. Vuorinen, *Intermetallics* **13**, 885 (2005).

[11] F. Faudot, A. Quivy, Y. Calvayrac, D. Gratias, M. Harmelin, *Mater. Sci. Eng. A* **133**, 383 (1991).

[12] Y.L. Cheung, K.C. Chan, Y.H. Zhu, *Mater. Charact.* **47**, 299 (2001).

[13] M.A. Suárez, R. Esquivel, J. Alcántara, H. Dorantes, J.F. Chávez, *Mater. Charact.* **62**, 917 (2011).

[14] E.V. Shalaeva, N.I. Medvedeva, *Philos. Mag.* **92**, 1649 (2012).

[15] G. Rosas, J. Reyes-Gasga, R. Perez, *Mater. Charact.* **58**, 765 (2007).